Journal of
Nanoscience and Nanotechnology
Vol. 10, 1584–1595, 2010

REVIEW

# Light Emission from Nanoscale Si/Si Oxide Materials*

G. G. Qin[1, 2, *], G. Z. Ran[2], K. Sun[2], and H. J. Xu[3]

[1] *Institute of Optoelectronic Materials and Technology, School for Information and optoelectronic Science and Engineering, South China Normal University, Guangzhou 510631, China*
[2] *State Key Lab for Mesoscopic Physics and School of Physics, Peking University, Beijing 100871, China*
[3] *School of Science, Beijing University of Chemical Technology, Beijing 100029, China*

Most porous Si materials studied have been oxidized in various degrees. The oxidized porous Si comprises of a great quantity of nanoscale Si particles (NSPs) and each of them is covered by a Si oxide layer. The structure and luminescence properties of the NSPs embedded Si oxide and the nanoscale Si/nanoscale $SiO_2$ multilayers are similar to those of the oxidized porous Si. All the three kinds of materials mentioned are called nanoscale Si/Si oxide materials and their photoluminescence and electroluminescence properties especially light emission mechanisms are reviewed in this article. Nanoscale Si/Si oxide materials have been well studied and are believed to be very promising Si based light emitting materials. The very distinct roles of the NSPs and the luminescence centers in Si oxide in the photoluminescence and electroluminescence from the nanoscale Si/Si oxide materials are highlighted.

**Keywords:** Nanosilicon, Si Photonics, Photoluminescence, Electroluminescence.

## CONTENTS



## 1. INTRODUCTION

Si is the most important semiconductor and electronic material. The technologies of Si materials and devices are highly mature and a state-of-the-art very large scale integration on Si has been scaled down to the sub-32 nm realm. In the information age, to realize ultra-high capacity information storage and transfer and ultra-high speed processing, there are pressing requirements to utilize photons instead of electrons as information carriers; correspondingly, the micro/nano electronic integration will develop into the micro/nano optoelectronic integration. The principal material in the electronic integration is Si and this status will continue throughout at least several following decades. What is the principal material for the optoelectronic integration? Will Si be? Despite the great success in the electronic integration, Si achieves limited progress as an optoelectronic material. After the Si optical modulation issue was overcome,[1] the Si light source issues became the unique bottleneck in Si photonics.[2, 3] Because of the indirect-band gap structure of Si, the light emitting efficiency of Si is very low. Since the discovery of strong visible photoluminescence (PL) from porous Si at room temperature by Canham in 1990,[4] "Si light emission" became a continuous and intensive research topic. Soon after 1990, several groups including our group

*Author to whom correspondence should be addressed.
*This is an invited review paper.



1533-4880/2010/10/1584/012 doi:10.1166/jnn.2010.2033

noticed that most porous Si materials are oxidized in various degrees,[5–8] and the oxidized porous Si materials comprise a great quantity of nanoscale Si particles (or other types of nanoscale Si) covered by Si oxide. Since then the nanoscale Si/Si oxide materials have been well studied and regarded as very promising Si-based light emitting materials. In 2000, Pavesi et al. first reported optical gain (of 100 $cm^{-1}$) from the Si NSPs embedded $SiO_2$ materials.[9] Electroluminescence (EL) with an external quantum efficiency in excess of 1% was achieved in the oxidized porous silicon.[10] This paper reviews PL and EL from the nanoscale Si/Si oxide materials including oxidized porous Si, nanoscale Si particles (NSPs) embedded Si oxide, and nanoscale Si/nanoscale $SiO_2$ multilayers. Revealing the mechanisms of Si light emission aims at enormously increasing the Si light emission efficiency and even at realizing electrically pumped Si lasers. In this paper, the mechanisms for both PL and EL from nanoscale Si/Si oxide materials and related debates have been discussed.

**G. G. Qin** was born in Nanjing, China in March 19, 1934 and graduated from the department of physics of Peking University, Beijing in 1956. He is now a professor in the school of physics of Peking University and South China Normal University and a member of the Chinese Academy of Sciences.

**G. Z. Ran** received his B.A. in Physics in 1991 from Henan University, M.sc. in 1996 from Zhengzhou University and Ph.D. Physics in 2001 from Peking University. Now he works as an associate professor of School of Physics of Peking University. His research interests are focused on semiconductor photonics, especially on Si photonics.

**Kai Sun** received his bachelor's degree from Peking University in 2004. Currently, he is a Ph.D. student in the Physics School of Peking University, under Professor Qin's supervision. His researches are focused on electronic device applications of Er-doped $Si/SiO_2$ system, novel Er-doped infrared materials and related energy transfer processes. He will receive his Ph.D. degree in Physics in July, 2009.

**Haijun Xu** received his B.Sc., M.Sc. and Ph.D. degrees from the Department of Physics, Zhengzhou University, China, in 2002, 2005 and 2008, respectively. He currently joins the Beijing University of Chemical Technology in 2008 as a lecturer, and his research is now focused on the physics of semiconductor optoelectronic material and devices.

REVIEW

REVIEW

## 2. THE MAINSTREAM PHOTOLUMINESCENCE MECHANISM MODELS FOR NANOSCALE Si/Si OXIDE MATERIALS

### 2.1. Light Emission from Nanoscale Si and the Quantum Confinement (QC) Model

The strong light emission from porous Si at room temperature, later shown to have a quantum efficiency as high as about 10%, found in 1990 was interpreted using the QC model:[4] the electron–hole pairs are generated inside the NSPs (or other types of nanoscale Si) and recombine there to emit visible light rather than the 1.1 $\mu$m infrared light, because the band gaps of the NSPs are widened compared to that of the bulk Si due to the QC effect. Just three months before the discovery of strong light emission from porous Si in 1990, Tagaki et al. reported room temperature PL from NSPs embedded Si oxide films prepared by microwave plasma, which was also interpreted by the QC model.[11] But at that time, their work did not receive much attention and nobody associated the PL from the NSPs embedded Si oxide with that from porous Si. In fact, using the QC model to explain the PL from nanosemiconductors can be dated back to 1970's. For example, Ref. [12] used the QC effect to discuss the PL blue shift for the GaAs/AlGaAs quantum wells in 1975 and Ref. [13] reported EL from the structure of Au/$SiO_2$/silicon-rich oxide (SRO)/$n$-Si and attributed the light emission to the NSPs, where the QC effect played a key role, in the SRO in 1984. The QC model achieved limited successes but encountered great difficulties in interpreting PL from porous Si. For examples, the QC model can hardly explain (1) the temperature dependence of the light emission wavelength.[14] (2) the large stokes shift between the light absorption and the light emission.[15] (3) light emission peak wavelength remained almost constant with change of NSP sizes.[16] (4) during oxidation of porous Si samples, diversity in wavelength shifts rather than uniformity in wavelength blue shifts of PL peaks was observed.[17–18]

The existence of a photoemission process inside the NSPs suggested by the QC model is unquestionable. The issue lies in whether NSPs play a dominant role in the photoemission process. Since 1992, many physical models for PL mechanisms of porous Si were proposed to challenge the QC model. According to an incomplete statistics by Canham, there were 24 mechanisms suggested between 1992 and 1997.[19] And a long-running debate began since then.

### 2.2. Light Emission from Luminescence Centers in Si Oxide and the Quantum Confinement/Luminescence Centers (QCLC) Model

According to the experiments, especially those can hardly be explained by the QC model, reported in literature and finished in our lab, we proposed in 1993 the luminescence centers (LCs) in Si oxide are dominant sources for light emission from porous Si, and suggested a novel physical model,[20] later called the quantum confinement/luminescence centers (QCLC) model, for the PL from nanoscale Si/$SiO_2$ materials containing porous Si. The main viewpoints of the QCLC model are as follows:

(1) After preparation, a porous Si sample put in air will be oxidized continuously until a stable state is reached. Therefore, most porous Si samples studied are oxidized in various degrees.

(2) Oxidized porous Si was simplified to a great quantity of NSPs (or other type of nanoscale Si) each covered wholly or partially by Si oxide.

(3) Photoexcitation occurs dominantly inside the NSPs, while photoemission occurs dominantly in the LCs (defects and impurities) in Si oxide adjacent to NSPs.

(4) Because of the indirect bandgap structure of the NSPs,[21,22] and low probability of band–band recombination there, through a quantum tunneling process, most electrons and holes photoexcited in NSPs enter the adjacent LCs in the Si oxide covering the NSPs, and recombine in the LCs to emit light. Figure 1, the original figure reported in Ref. [20], shows photoexcitation occurs inside the NSPs and photoemission occurs in the LCs in Si oxide and electrons and holes in NSPs tunnel into the LCs in Si oxide.

(5) The QCLC model claims that light emissions with different wavelengths originate from different types of LCs in Si oxide. As a contrast, the QC model claims that light emissions with different wavelengths originate from NSPs with different sizes.

(6) For a PL spectrum of a porous Si sample with several peaks, it is very difficult to identify which kind of LCs (defects or impurities) is responsible for a concrete peak in

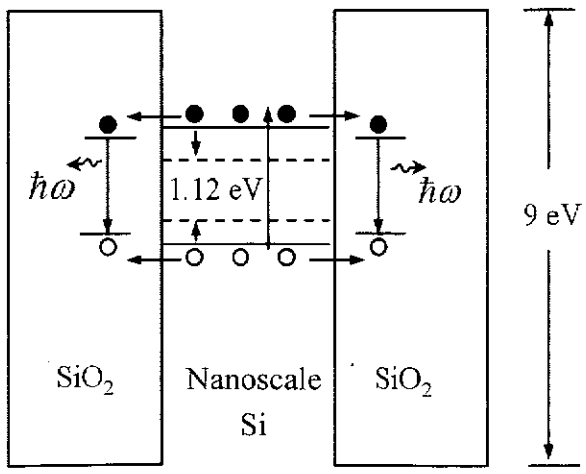


**Fig. 1.** Schematic illustration of electrons and holes tunneling into the luminescence centers in the $SiO_2$ layer to emit light. Reprinted with permission from [20], G. G. Qin and Y. Q. Jia, *Solid State Commun.* 86, 559 (**1993**). © 1993, Elsevier.

the PL spectrum. Ref. [20] proposed that the non-bridging oxygen hole centers might be the LCs responsible for the ~1.9 eV PL peak for porous Si.

(7) Because both the oxidized porous Si and NSPs embedded Si oxide comprise a great quantity of NSPs covered by Si oxide, and have similar PL spectra, it was suggested that the two materials have a common PL mechanism and the QCLC model can be applied.[20]

Also in 1993, Prokes proposed independently that the light emission from porous Si originates from the LCs in Si oxide, but did not discuss the roles of the NSPs.[23]

Here, some experimental examples which can be well explained by the QCLC model rather than by the QC model are given:

(1) Because the QCLC model claims that light absorption and light emission occurs in two different subjects, the NSPs and the LCs in the Si oxide adjacent the NSPs, respectively, the model can easily explain the large Stokes shift observed.[15, 20]

(2) The QCLC model can easily explain the experimental facts that the PL peak wavelength remained almost constant when the sizes of the NSPs are changed, because the LC energies are generally independent of the sizes of the NSPs.

(3) The QCLC model can explain the diversity of the PL peak shifts with temperature. Because temperature dependence of energies of the LCs in Si oxide is generally very weak, if only one kind of LCs is responsible for a PL peak, then the fact that the PL peak almost does not shift with the temperature can be interpreted. If two or more than two kinds of LCs are responsible for a PL peak, and the intensities of light emissions from these LCs have different temperature dependence relations, the PL peak will shift, generally. If the PL intensity of the LCs with higher energy increases faster or decreases slower when temperature is raised, the PL peak will blue shift, otherwise, red shift.

(4) The PL peak positions for a lot of porous Si samples just fabricated in different conditions are quite different in wavelength. When oxidized, because the sizes of all the NSPs in the porous Si samples will decrease, the PL peak wavelengths for all the porous Si samples should blue shift according to the QC model. However, the experimental results are that the PL peaks from the porous Si samples converged to almost the same position, ~1.7 eV, by blue shift, red shift, or no shift.[17, 18] The interpretation of the QCLC model for this result is like that after sufficient oxidation of the porous silicon, one kind of stable LCs in the Si oxide with a photon energy of ~1.7 eV (or several kinds of stable LCs in the Si oxide with photon energies close to ~1.7 eV) dominates the light emission process.

Most recently, for the nanoscale $Si/SiO_2$ materials, in order to classify the origins of PL from either LCs or NSPs, Ref. [24] used low temperatures (85 K) pulsed high-field magneto-PL (50 T) experiments to directly probe the extent of the wavefunction responsible for the PL. They concluded that defects are generally the dominant source for light emission. The principle of this novel method is like that the applied magnetic field has an associated length scale, $l = (h/2\pi eB)^{1/2}$, where $h$ is the Planck constant and $e$ is the electron charge, which acts to confine the wavefunction of the state under study before recombination, and hence increases the PL energy.[25, 26] Such a method can distinguish between a state confined to a few nanometers within a Si nanocrystal and a highly localized defect state. The PL energies for LCs are independent of the magnetic field as shown in Figure 2(a); after the LCs are passivated, the PL energies for the NSPs increase as the magnetic field is raised as shown in Figure 2(b). Such a method is able to distinguish the light emission process occurring in NSPs from that in LCs in Si oxide, but seems to have a restriction for such a nanoscale $Si/SiO_2$ system, where the NSPs are very small and the LCs are large (e.g., a cluster of defects) and they have near sizes.

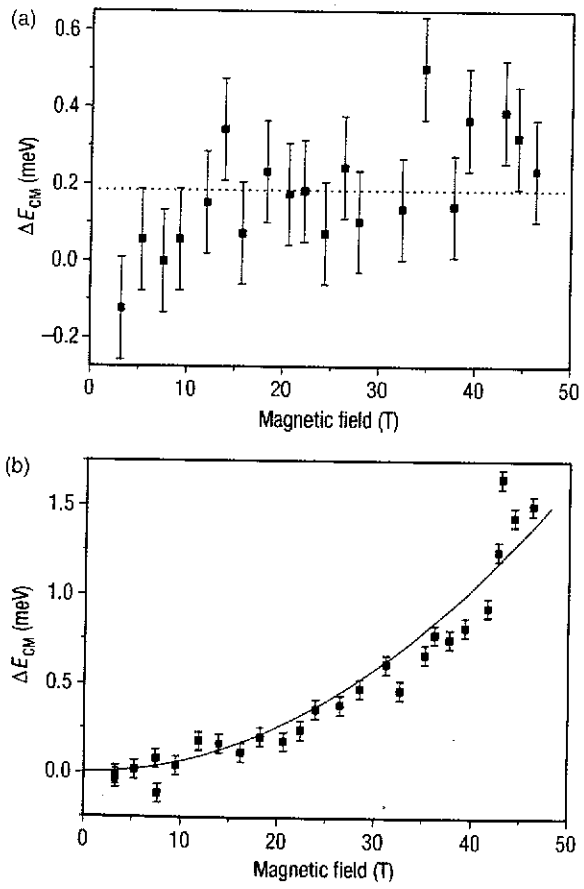


**Fig. 2.** Shift of the centre of mass of the PL peak ($\Delta E_{CM}$) as a function of magnetic field at 85 K. (a) Data for the as-crystallized sample. The dotted line indicates the mean value of $\Delta E_{CM}$. (b) Data for the passivated sample. The solid line shows the parabolic fit. Reprinted with permission from [24], S. Godefroo et al., *Nat. Nanotechnol.* 3, 174 **(2008)**. © 2008, NPG.

REVIEW

## 3. IN WHAT CASES THE NANOSCALE Si PARTICLES OR THE LUMINESCENCE CENTERS IN Si OXIDE DOMINATE IN LIGHT EMISSION

### 3.1. Viewpoints

In nanoscale Si/Si oxide materials, in most cases, one of the two factors, either the NSPs or the LCs in Si oxide, predominates in light emission and takes priority over the other, then considering only the dominant factor is sufficient. However, the viewpoints on the issue that in a concrete case which factor is the dominant one are controversial. In 1994, Cullis et al. pointed out that in the abstract of Ref. [27] "Crystalline Si nanostructures ... account for its 750 nm red photo and cathodluminescence... . The luminescence properties of Si oxide are of paramount importance in interpreting the many additional (shorter wavelength) emission bands observed." In 1997, they elucidated this viewpoint more clearly: red PL of porous Si originates from NSPs, and "As with the blue-green $F$-band, the UV bands are only observed from oxidized layers and are likely also to arise from the defective oxide phase."[28] In 1999, Wolkin et al.[29] reported that when NSPs are larger than ~3 nm, the QC effect alone can explain most their PL results, when the NSPs are small enough (from the figures in Ref. [29], smaller than about 1.6 nm), light emission originates from the Si=O double bonds at the NSP/Si oxide interface. But we are suspicious of the conclusions. First, their porous Si sample was oxidized at room temperature only for 24 hrs, and it was thought that this oxidation time had been long enough for getting a stable PL.[29] However, in the experiments of Ref. [17], in order to get a stable PL when oxidation was performed at even 200 °C, the oxidation time should be as long as 200 hrs; while oxidized at room temperature, the oxidation time should be longer than a year. Secondly, the conclusion of Ref. [29] seems contrary to the Heisenberg uncertainty relation. According to the uncertainty relation $\Delta x \cdot \Delta p \geq h/4\pi$, the smaller the NSPs, that is, the smaller the $\Delta x$, the larger the uncertain moment of $\Delta p$, and the more beneficial for recombination of the electron–hole pairs in the NSPs with indirect band gaps to emit light.

Based on the theoretical work jointly finished by G. Qin, Wang and our group,[30,31] we developed a PL theory considering both the QC and the QCLC processes. The probabilities of these two processes were quantitatively compared, and the answers for what physical factors determine the probabilities of the QC and the QCLC processes, and for what conditions under which the QC or the QCLC process dominates, were given.[32] Suppose that a NSP is a cubic with side length of $L$, and there is no NSP with side length smaller than $L_0$, that is, $L_0$ is the smallest side length of the NSPs, and when $L$ is larger than $L_0$, the size profile obeys the Gaussian function.

$$\rho(L) = \frac{1}{\sigma\sqrt{2\pi}} \exp\left[-\frac{(L-L_m)^2}{2\sigma^2}\right] \quad (1)$$

where $L_m$ is the most probable size, $\sigma$ the root mean-square deviation. Suppose further that the effective-mass approximation holds. Some additional assumptions can be seen in Ref. [32]. Denote the probabilities of the QC and the QCLC processes as $P_{QC}$ and $P_{QCLC}$, and the average values of the $P_{QC}$ and the $P_{QCLC}$, in the NSP size distribution mentioned above, as $\langle P_{QC}\rangle$ and $\langle P_{QCLC}\rangle$. $\langle P_{QC}\rangle$ is determined by $L_m$, $L_0$, and $\sigma$, the size parameters of NSPs, and $\langle P_{QCLC}\rangle$ is determined not only by the NSP parameters, but also by the LC parameters, $N_{LC}$, $\sigma_0$ and $\eta_{LC}$, where $N_{LC}$ is the density of the LCs, $\sigma_0$ the bigger one in the hole- and electron- capture-cross-sections, and $\eta_{LC}$ the radiative recombination probability of the electron–hole pairs in the LCs. Supposing that both $\sigma$ and $L_0$ have definite values and that there is only one kind of LCs, which have definite $\sigma_0$ and $\eta_{LC}$, then $L_m$, $N_{LC}$ are the two variable parameters. And a critical curve, on which $\langle P_{QC}\rangle$ equals to $\langle P_{QCLC}\rangle$ at each $(L_m, N_{LC})$ point, on the $L_m$ ($X$-axis)–$N_{LC}$ ($Y$-axis) diagram can be obtained from the theory.[32] In the top right region of the critical curve on the $N_{LC}$–$L_m$ diagram as shown in Figure 3, $\langle P_{QCLC}\rangle$ is larger than $\langle P_{QC}\rangle$, that is, the QCLC process dominates the QC process; while in the bottom left region of the critical curve, $\langle P_{QC}\rangle$ is larger than $\langle P_{QCLC}\rangle$, that is, the QC process dominates the QCLC process. A certain nanoscale Si/Si oxide material with definite $L_m$ and $N_{LC}$ corresponds to a definite $(L_m, N_{LC})$ point in the $N_{LC}$–$L_m$ diagram. If this point locates in the QC-dominating region, the QC process dominates, and the farther this point away from the critical curve, the more the QCLC process dominates. In Figure 3, the $(L_m, N_{LC})$ points corresponding to the nanoscale Si/Si oxide materials with a constant $N_{LC}$ but varying $L_m$ locate in a line parallel to $X$-axis. When $L_m$ is large enough, the

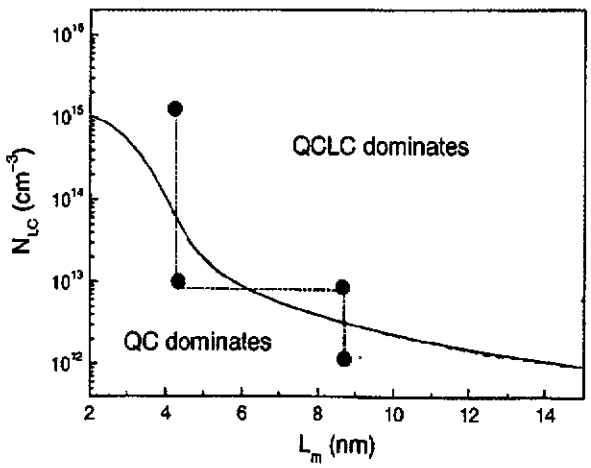


Fig. 3. A critical curve and the two regions where the quantum confinement process and quantum confinement luminescence centers process play a major role. Adapted with permission from [32], G. G. Qin and Y. J. Li, *Phys. Rev. B* 68, 085309 (**2003**). © 2003, AIP.

($N_{LC}$, $L_m$) point locates in the QCLC-dominating region. When $L_m$ decreases, after crossing the critical curve, it enters the QC-dominating region. In other words, decreasing the sizes of the NSPs to a certain degree will cause the QC process to surpass the QCLC process. It seems that this conclusion is contrary to that in Ref. [29], but consistent with the uncertainty relation. In Figure 3, the ($L_m$, $N_{LC}$) points corresponding to the nanoscale Si/Si oxide materials with a constant $L_m$ but varying $N_{LC}$ locate in a line parallel to the $Y$-axis. When $N_{LC}$ is low enough, the ($N_{LC}$, $L_m$) point locates in the QC-dominating region. When $N_{LC}$ increases, after crossing the critical curve, it enters the QCLC-dominating region. In other words, increasing $N_{LC}$ to a certain degree will cause the QCLC process to surpass the QC process.

The critical curve locating in the $N_{LC}$–$L_m$ diagram can hardly be determined exactly from theory, because not only in the theory several approximations have been applied, but also getting the precise values for some parameters of NSPs and LCs is difficult. However, the theory in Ref. [32] has a realistic meaning for improving luminescence efficiency of nanoscale Si/Si oxide materials. According to the theory, in order to increase luminescence efficiency, in the QCLC-dominating region, the carries capture cross-sections, radiative recombination probability, and especially the density of the LCs should be increased as far as possible. In the QC-dominating region, the smaller the sizes of NSPs, the higher the luminescence efficiency. Just as emphasized in Section 2.2, in most nanoscale Si/Si oxide materials, light emission from the LCs in the Si oxide adjacent to the NSPs dominates that from the NSPs. Nevertheless, on the basis of the theory in Ref. [32], it is concluded that decreasing the sizes of NSPs and/or the densities of the LCs in Si oxide sufficiently, light emission from NSPs may dominate that from LCs in Si oxide.

### 3.2. Experimental Evidence

Great experimental efforts have been devoted to classify the two competitive processes in PL from the nanoscale Si/Si oxide materials in recent years. Wang et al. systematically studied the PL from the nanoscale Si/$SiO_2$ materials prepared by chemical vapor deposition.[33] Room-temperature PL spectra of the materials with different Si concentrations annealed at 1150 °C for 1 h in $N_2$ ambient are shown in Figure 4. They found that each PL spectrum for the materials comprised of three Gaussian peaks named A, B, and C. The wavelength of the peak A is temperature dependent and NSP size dependent, but the peak B is not. It is concluded that the peak A originates from the QC effect in NSPs and the peak B originates from the radiative recombination of the localized levels of the interface states between NSPs and the $SiO_2$ matrix or from defect-related centers in the $SiO_2$ matrix. Using a high resolution transmission electronic microscope, they found the sizes of the

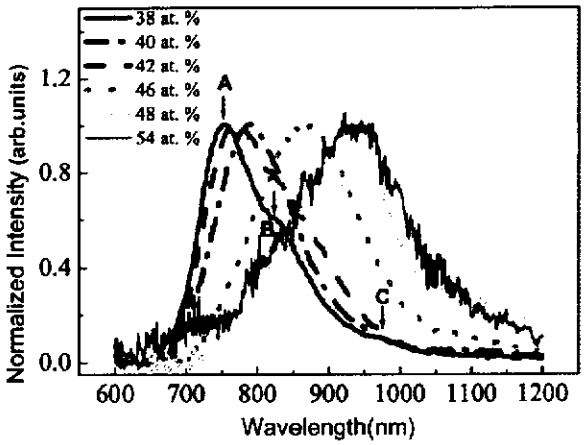


**Fig. 4.** A comparison of room-temperature PL spectra of samples with different Si concentrations annealed at 1150 °C for 1 h in $N_2$ ambient. The approximate positions of peak *A*, *B*, and *C* are denoted by arrows. Adapted with permission from [33], X. X. Wang et al., *Phys. Rev. B* 72, 195313 (**2005**). © 2005, APS.

NSPs increased with increasing the Si content in the sample. They showed how the peak intensity ratio of the peak A to the peak B decreased with increasing sizes of NSPs (increasing the Si content), as shown in Figure 5, which supported strongly the theoretical prediction in Ref. [32]: the larger the size of NSPs, the more beneficial for the LC (the interface state) emission process to surpass the NSP emission process.

In Ref. [34], a new type of porous Si material, Si nanoporous pillar array (Si-NPA) composing micron-sized quasi-identical Si pillars was prepared. In the Si pillars, there are dense nanopores. High resolution transmission electronic microscope analysis showed the Si pillars comprise a great quantity of surface-oxidized NSPs with sizes from ~1.95 nm to ~4.4 nm.[34] The room temperature PL spectra excited at varying wavelength are depicted in Figure 6(a). Fitting each spectrum by the Gauss–Newton method, the peak positions of the three emission bands determined are ~420, ~640 and ~705 nm. The first one is

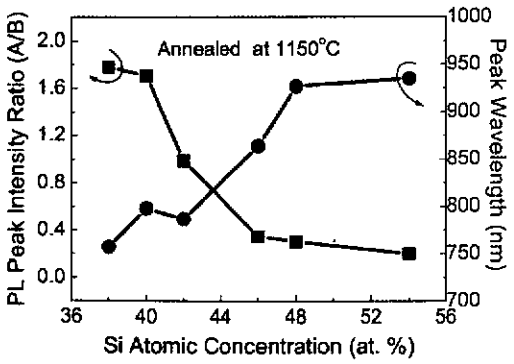


**Fig. 5.** PL peak intensity ratio of peak *A* to *B* and peak wavelength as a function of Si concentration in NSPs embedded $SiO_2$ films. The sample was annealed at 1150 °C. Reprinted with permission from [33], X. X. Wang et al., *Phys. Rev. B* 72, 195313 (**2005**). © 2005, APS.

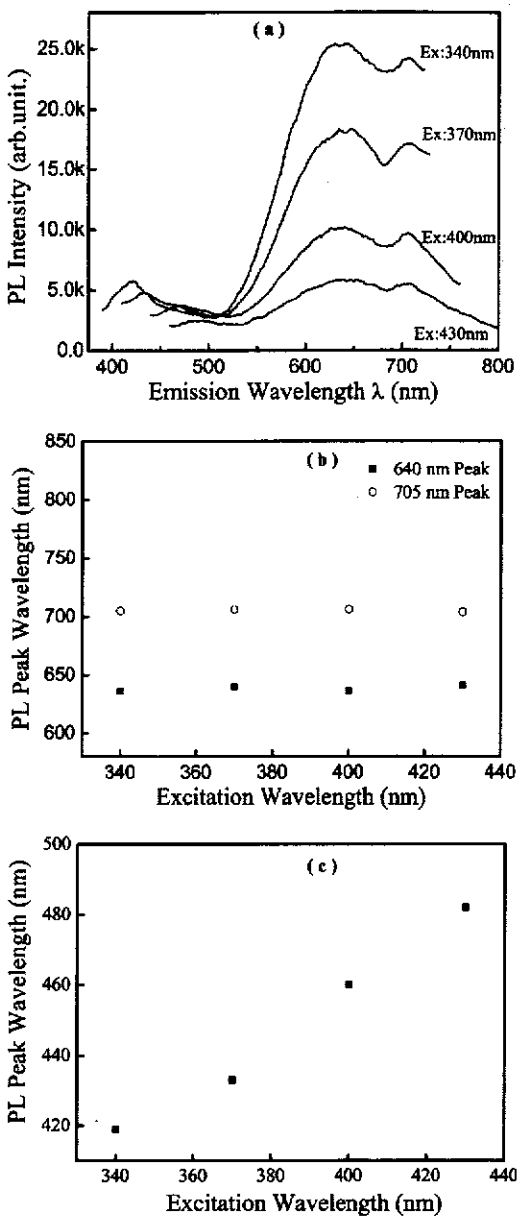


**Fig. 6.** (a) PL spectra of Si-NPA measured at several excitation wavelengths. (b) the PL peak wavelengths as functions of excitation wavelength for the two red emission bands, and (c) that for the blue emission band. Adapted with permission from [34], H. J. Xu and X. J. Li, *Opt. Express* 16, 2933 (**2008**). © 2008, OSA.

in the blue range and the other two in the red range. Evolution of the PL peak positions with excitation wavelength was shown in Figure 6(b, c). As the excitation wavelength increases, the peak intensities of the two red PL bands decrease monotonously, while the peak positions as well as the full width at half maximum (FWHM) remain almost unchanged (Fig. 6(b)). This evolution of PL peak wavelengths and FWHM directly ruled out the possibility that the two red PL bands originate from the QC process, but could be well explained by the QCLC process: the emission process mainly occurs through the LCs in the Si oxide layers adjacent to the NSPs.[32] Considering that the energy levels of the LCs are generally independent of the sizes of NSPs or the excited wavelengths, the peak positions and the FWHM of the two red emission bands remain unchanged when excited by different wavelength light. As to the evolution of intensities for the two red PL bands and the blue PL band, which could be explained by either the QCLC process or the QC process as follows: the photoexcitation process occurs in the NSPs, but only the NSPs with energy gaps smaller than the excitation photon energies could be effectively excited, therefore peak intensities will decrease monotonously with increasing excitation wavelength.

As for the blue emission band, with excitation wavelength increasing the PL peak wavelength increases monotonously (Fig. 6(c)). Moreover, the gap energy evaluated in theory is well in accordance with the peak energy of the blue emission band observed in Si-NPA.[34] Because in the QC process both photoexcitation and photoemission occur in NSPs, the evolution of the PL peak wavelength with excitation wavelength changing for the blue PL band is in accord with the QC process.

The PL excitation spectra of Si-NPA were measured by setting the monitored wavelengths at 420, 640 and 705 nm, as depicted in Figure 7. It was found that the three PL excitation spectra exhibit peak positions almost the same (around 370 nm). The experimental results can be explained by photoexcitation in NSPs. Moreover, there are large Stokes shifts between photoexcitation energies and photoemission energies for the PL excitation with monitored wavelengths at 640 and 705 nm. Using the QCLC model, the large Stokes shifts can be explained by that photoexcitation in NSPs and photoemission occurs in LCs, and the energy differences between the energy gaps of NSPs and the light emission energies for the 640 and 705 nm LCs are large.

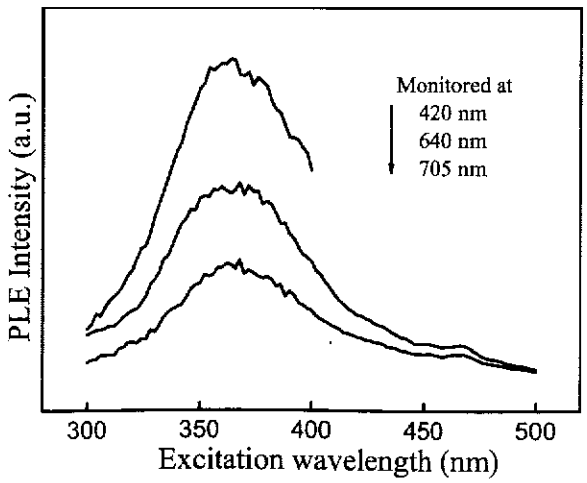


**Fig. 7.** The PL excitation spectra of Si-NPA taken under three different monitored emission wavelengths. Reprinted with permission from [34], H. J. Xu and X. J. Li, *Opt. Express* 16, 2933 (**2008**). © 2008, OSA.

### 3.3. Other PL Processes in the Nanoscale $Si/SiO_2$ Materials

In both the QC and QCLC processes, photoexcitation occurs in the NSPs. However, in NSPs/$SiO_2$ materials, when the NSPs vanish, e.g., by oxidizing at high temperatures above 1150 °C,[35] the PL intensity generally decreases substantially rather than disappears entirely. In Ref. [36], when a porous Si sample with a blue-light PL band was oxidized for half an hour at 1150 °C, the NSPs inside the porous Si sample disappeared, but the PL intensity reduced to about 30% rather than zero. And the PL excitation spectrum of the sample changed into a spectrum very similar to that of Si oxide. These experimental results indicate that a PL process (or PL processes) with the photoexcitation process independent of NSPs exists. In oxidized porous Si, Ref. [37] reported three PL peaks in the ultraviolet range with peak positions (340, 350, and 370 nm) very close to those of $SiO_2$ powder. The PL excitation spectrum shown in Figure 8(a) for the oxidized porous Si without NSPs (labeled by $O_2$ 1150 °C) is very similar to that of the $SiO_2$ powder shown in Figure 8(b), but very different from those of the oxidized porous Si with NSPs (labeled by $N_2$ 1150 °C and $O_2$ 1000 °C) as shown in Figure 8(a). It was concluded that in oxidized porous Si there is a PL process, very similar to that in Si oxide, in which both photoexcitation and photoemission occur in Si oxide. According to these experiments, it was suggested that besides the QC and the QCLC processes, there is a third PL process: photoemission takes place in the LCs in Si oxide, while photoexcitation occurs in the Si oxide, perhaps in the same LCs.[38] Most recently, Ref. [39] studied PL of erbium-doped SRO samples. From their experimental results, a LC-mediated excitation process was suggested.

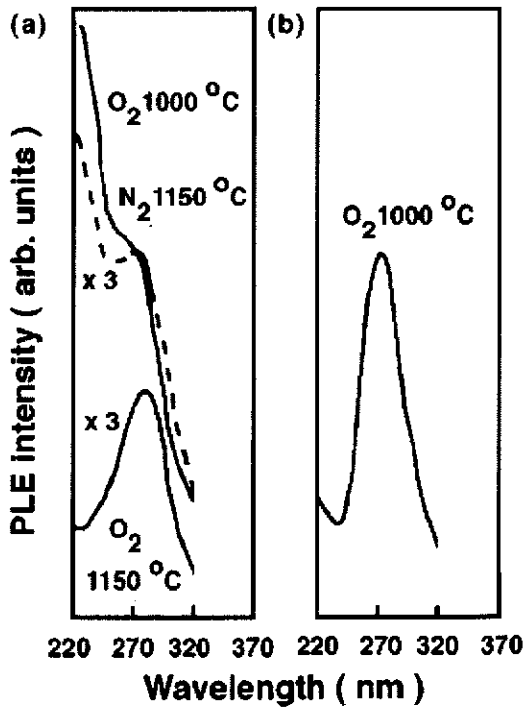


**Fig. 8.** The PL excitation spectra monitored at 370 nm for the porous Si samples which have been (a) (1) oxidized at 1000 °C for 1 min, (2) oxidized at 1000 °C for 1 min first and then annealed in $N_2$ at 1150 °C for 5 min, and (3) oxidized at 1000 °C for 1 min first and then at 1150 °C for 5 min and (b) $SiO_2$ powder annealed at 1000 °C for 1 min. Reprinted with permission from [37], G. G. Qin et al., *Appl. Phys. Lett.* 69, 1689 (**1996**). © 1996, AIP.

## 4. ELECTROLUMINESCENCE FROM NANOSCALE Si/Si OXIDE STRUCTURES

### 4.1. Early Studies

In 1984, Dimaria et al.[13] reported visible EL from $SiO_2$ films containing tiny Si islands in a structure of Au/$SiO_2$ (50 nm)/SRO (20 nm)/*n*-Si. The EL was explained by the inter-band transition in the tiny Si islands in the SRO and where the QC effect plays a vital role. The visible EL from porous Si was reported first by Ritcher et al. in 1991.[40] Koshida and Koyama[41] reported a stable EL from the structure of semitransparent metal/porous Si layer/*p*-Si in 1992. Both the above studies and some other early studies on the EL from porous Si[42–46] all ascribed the EL to light emission from the NSPs (or other types of nanoscale Si) and the QC effect.

### 4.2. The Role of Luminescence Centers in Si Oxide in Nanoscale Si/Si Oxide Electroluminescence

In 1994, we observed EL from a structure of semitransparent Au/native Si oxide/*p*-Si (5–10 Ωcm) under a forward bias of larger than 4 V.[47] We noticed that its spectra are very similar to that of the semitransparent Au/porous Si/*p*-Si (5–10 Ωcm) also made in our laboratory. Both their EL peaks are close to ~700 nm, as shown in Figure 9. This implies the native Si oxide (with a thickness of only ~2 nm) plays a similar function as the oxidized porous Si with a great quantity of NSPs covered by Si oxide and hence the NSPs are not essential for the EL. After the native Si oxide layer on the *p*-Si was removed, a semitransparent Au film was deposited on the bare *p*-Si surface, no EL could be observed from the resulting structure of Au/*p*-Si. This experimental result indicates that the native Si oxide plays a key role in EL from the semitransparent Au/native Si oxide/*p*-Si structure. We proposed that the EL originates from the LCs (defects) in the native Si oxide.[47] As far as we know, it was for the first time to point out that EL can originate from the LCs in Si oxide. The EL mechanism for the forward biased Au/native Si oxide/*p*-Si is explained as follows. Under forward bias, the electrons in the Au film and the holes in the *p*-Si tunnel into the LCs in Si oxide, and then recombine there to emit

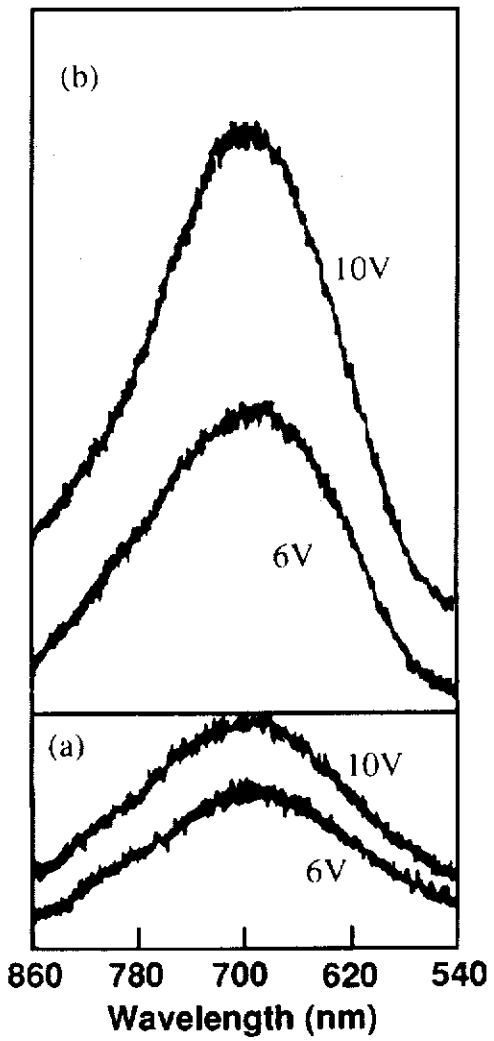


**Fig. 9.** EL spectra for the semitransparent Au/native Si oxide/p-Si and the semitransparent Au/porous Si/*p*-Si. Reprinted with permission from [47], G. G. Qin et al., *Superlatt. Microstruct.* 16, 387 (**1994**). © 2000, AIP.

light. Supposed further that the EL from the semitransparent Au/porous Si/*p*-Si originates dominantly from the LCs in the Si oxide covering the NSPs rather than from the NSPs themselves in the porous Si, the similarity in the EL spectrum of the Au/native Si oxide/*p*-Si and that of the Au/porous Si/*p*-Si can be realized. In order to study the role of the NSPs in Si oxide on the EL, 3–12 nm SRO film was deposited to replace the native oxide layer and the EL from the semitransparent Au/SRO/*p*-Si was systematically studied.[48]

The viewpoints that EL can dominantly originate from the LCs in Si oxide have been supported by many experiments. For examples: dependence of the EL peak position on the work function of the metal in the EL structure of semitransparent metal/SRO/*p*-Si,[49] the $\gamma$-ray radiation effect on the EL spectra,[50] and similarity of the EL spectra of the Au/NSPs embedded Si oxide/*p*-Si and the Au/nanoscale Ge particles embedded Si oxide/*p*-Si.[51] In the EL study on the semitransparent Au/Si ions implanted $SiO_2$/*p*-Si structure, Liao et al. did not observe any red shift of the EL spectra with increasing annealing temperature and hence ascribed the EL origin to the LCs rather than the NSPs in Si oxide.[52] The work presented by Yuan et al. on EL from native $SiO_2$ [53] and on spark-processed silicon[54] provided strong supports to the conclusion that LCs in Si oxide are the dominant origin of EL. Heikkila et al. studied EL from several $SiO_2$–Si layer structures grown on silicon and metal substrates.[55] Their experimental results indicated that significant EL emission can be observed only in those samples that have $SiO_2$/*p*-type crystalline Si interface. The most promising explanation of this phenomenon is that there are defect levels in the thin Si oxide layer near the interface.[55] The EL studies on the structures of depositing Al-doped silicon oxide film[56] and Ge nanocrystal embedded Si oxide film[57] on *p*-Si substrates indicated that in both cases, the EL spectra centered at 510 nm could be ascribed to the defects in the Si oxide films.

A common deficiency in most experiments for EL from nanoscale Si/Si oxide structures is that the shapes and sizes of the NSPs are not uniform and hardly controllable. In order to improve this situation, EL from the semitransparent Au/nano-sandwich of ($SiO_2$/Si/$SiO_2$)/*p*-Si structure was studied.[58,59] Twenty-one devices with this structure were prepared, where the left and right $SiO_2$ layers had definite thicknesses of 3 and 1.5 nm, respectively, and the nano-Si layer in the sandwich a thickness in a range of 1–5 nm with an interval of 0.2 nm.[59] A control device with the semitransparent Au/$SiO_2$ (4.5 nm)/*p*-Si structure that has not any nano-Si layer was also prepared. It is found that the current (Fig. 10(a)), EL peak wavelength (Fig. 10(b)) and EL intensities (Fig.10(c)) of these devices oscillate synchronously with increasing nano-Si layer thickness. If the nano-Si layer is the dominant origin of the EL, the EL peak wavelength of the devices should monotonically redshift with increasing nano-Si layer thickness, and the control device without any nano-Si layer should have little EL. These predictions are not consistent with the experimental facts. In fact, the EL spectrum of each device can be decomposed into two Gaussian bands with peak energies of 1.82 and 2.25 eV. The current and the intensities of these two bands oscillate synchronously when the nano-Si layer thickness increases. As a result, the intensity of the EL peak composed of the two Gaussian bands oscillates synchronously. The oscillation period was shown theoretically to be half a de Broglie wavelength of the carriers (0.4 ~ 0.6 nm), which is consistent with the experimental value (0.5 nm).[59] The experimental results indicate that the EL originates dominantly from two types of LCs with energies of 1.82 and 2.25 eV in the $SiO_2$ barriers, rather than from the nano-Si well in the nano-sandwich of ($SiO_2$/Si/$SiO_2$).

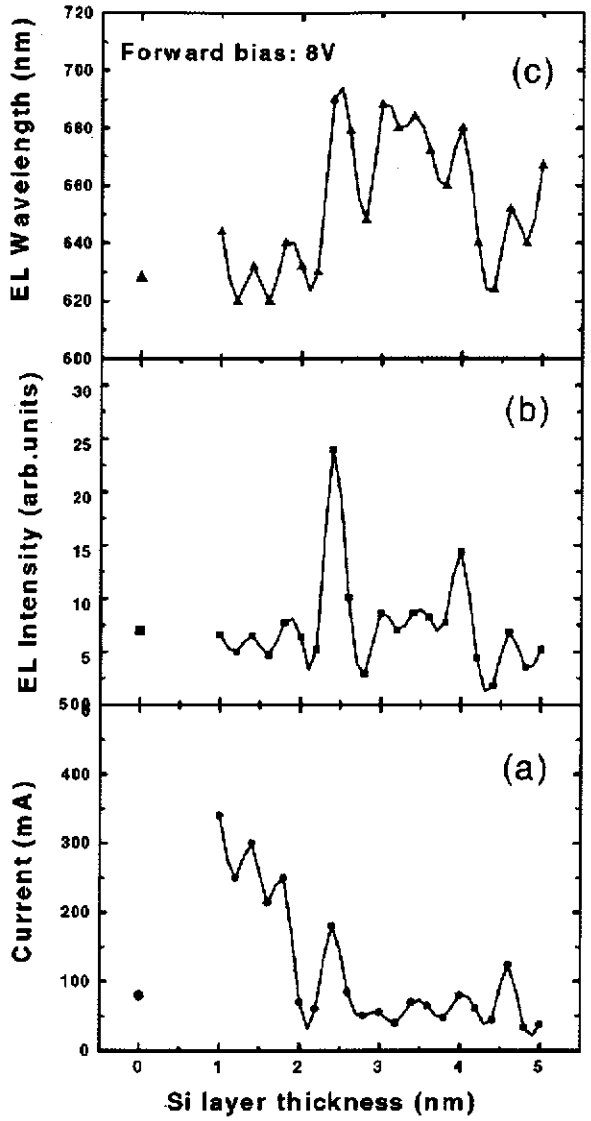


**Fig. 10.** (a), (b) and (c), show, respectively, the currents, EL intensities and peak wavelengths of the Au/nano-sandwich of $(SiO_2/Si/SiO_2)/p$-Si structure under a forward bias of 8 V as functions of the Si layer thickness in the range 1–5 nm. The same parameters of the control device without any Si layer under the same bias are also shown. Reprinted with permission from [59], G. G. Qin et al., *J. Phys.: Condens. Matter.* 13, 11751 (**2001**). © 2000, AIP.

### 4.3. The Role of Nanoscale Si Particles in Nanoscale Si/Si Oxide Electroluminescence

Though the early studies ascribed the EL from nanoscale Si/Si oxide to the QC effect of nanoscale Si, solid and direct experimental evidence, which demonstrated quantitatively dependence of EL wavelength on the size of nanoscale Si consistent with the predication of the QC effect, is still lacking. Nevertheless, nanoscale Si has really important effects on EL from nanoscale Si/Si oxide through affecting the light emission from LCs and/or conductance of the EL structures. In the studies how the light emission from the LCs in Si oxide is affected by NSPs, the $Er^{3+}$ LCs have been paid most intensive attention, because the 1.54 $\mu$m light emission from $Er^{3+}$ is just located in the major window of fiber telecommunication. A great enhancement of the $Er^{3+}$ PL at 1.54 $\mu$m due to the NSPs in Er doped SRO was demonstrated[60] in 1997. The NSPs was also demonstrated to be beneficial for electric transport in the Er doped SRO.[61] Enhancement of $Er^{3+}$ EL by nanoscale Si was demonstrated in the structure of $Au/SiO_x$:Si:Er/$n^+$-Si under reverse bias.[62,63] Comprehensive summaries on EL from Er-doped Si nanostructures can be found in Refs. [64 and 65]. Recently, some notable progresses were achieved in the studies for EL from Er doped Si oxide.[66–69]

The effects of NSPs on the $Er^{3+}$ EL from the SRO: Er films deposited by the magnetron sputtering technique have been studied.[70] The compositions of the films were denoted by $Er:Si_{1+x}O_2$ with $x$ quantifying the degree of Si richness. The $x$ in experiments was taken as 0, 0.60, 1.85, 2.00, 2.64, or 4.50. Figure 11 shows that the forward-biased $I$–$V$ relations of the ITO/$Er:Si_{1+x}O_2/p$-Si structures with $Er:Si_{1+x}O_2$ having the six $x$ values present good linearity in a log–log plot with an average slope of 1.87 near to 2. It can be well explained by the space-charge- limited- current mechanism, in contrast with the Fowler-Nordheim hopping mechanism usually seen in the hot-electron-impact EL. The main transport mechanism is considered to be hopping between NSPs, between a NSP and a trap state, and between trap states. Figure 11 shows that the conductivity of the $Er:Si_{1+x}O_2$ films with $x = 4.5$ is enhanced by six times compared to the conductivity of $Er:SiO_2$.

Figure 12 shows the dependence of PL and EL efficiencies on the degree of Si richness. The most noticeable feature is the two orders enhancement in the EL efficiency while the degree of Si richness $x$ is optimum ($x = 2$), which clearly demonstrates the sensitization effect of NSPs

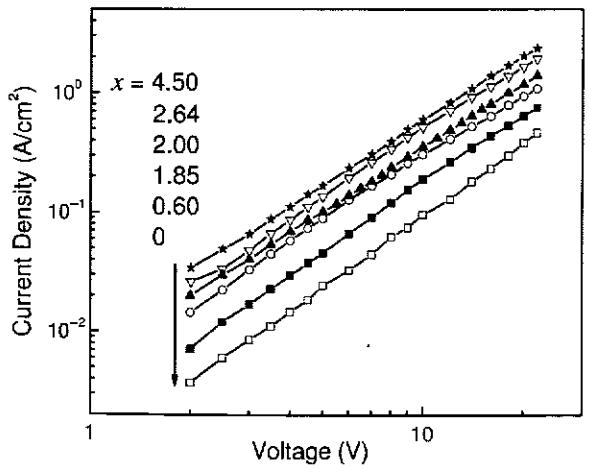


**Fig. 11.** $I$–$V$ characteristics of the forward-biased diodes having a structure of ITO/$Er:Si_{1+x}O_2/p$-Si with $x = 0$, 0.60, 1.85, 2.00, 2.64, and 4.50 on a log–log plot. Reprinted with permission from [70], K. Sun et al., *Nanotechnology* 19, 105708 (**2008**). © 2008, IOP.

REVIEW

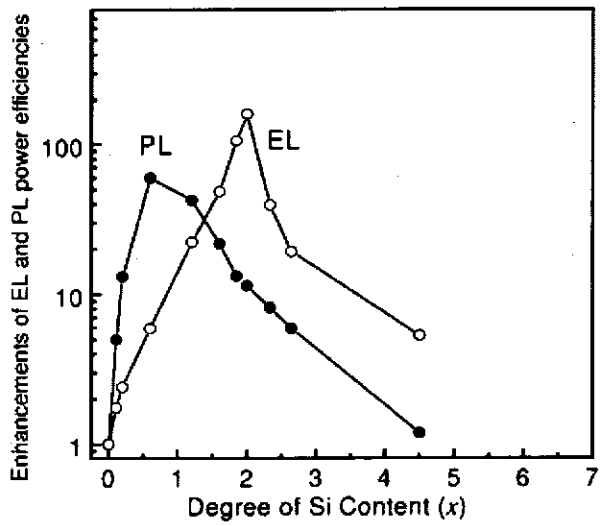


Fig. 12. Enhancements of $Er^{3+}$ EL (o) and PL (•) power efficiencies of ITO/Er:$Si_{1+x}O_2$/p-Si diodes and Er:$Si_{1+x}O_2$ films, respectively, as functions of degree of Si richness, $x$, compared to those with $x = 0$. The lines are drawn to guide eyes. Adapted with permission from [70], K. Sun et al., *Nanotechnology* 19, 105708 (**2008**). © 2008, IOP.

REVIEW

on the $Er^{3+}$ EL. When $x$ becomes larger than 2, the EL efficiency decreases suddenly. It can be attributed to coalescence of NSPs. Actually, if we assume the NSPs are uniform in size and assembled by random close packing, the degree of Si richness for the coalescence can be calculated to be around 2.4.[71] Another feature in Figure 12 is the large difference between the optimal degree of Si richness for PL efficiency and that for EL efficiency. This large disparity in optimal $x$ reflects the different roles for NSPs in the PL and EL processes.

## 5. CONCLUSIVE REMARKS

In the nanoscale Si/Si oxide materials, both the NSPs and the LCs in Si oxide are the key factors for PL and EL. In PL, in most cases, the LCs in the Si oxide adjacent to the NSPs dominate the photoemission process, while the NSPs play a major role in photoexcitation. Decreasing the sizes of NSPs especially the densities of the LCs in Si oxide, the photoemission in NSPs may exceed that in LCs in Si oxide to play the major role in PL. As for EL from the nanoscale Si/Si oxide structures, much more direct evidence for light emission from LCs rather than from NSPs has been adduced. The NSPs in Si oxide can increase the electrical conductance of the EL structures, and can enhance the EL intensity greatly through promoting the light emission from the LCs in Si oxide in the EL structures.

**Acknowledgment:** This work was supported by the National Natural Science Foundation of China (No. 50732001; 10874001; 10674012; 60877022) and National Basic Research Program of China (973 Program, No. 2007CB613401).

## References and Notes

1. A. Liu, R. Jones, L. Liao, D. Samara-Rubio, D. Rubin, O. Cohen, R. Nicolaescu, and M. Paniccia, *Nature* 427, 615 (**2004**).
2. G. T. Reed and A. P. Knights, Silicon Photonics: An Introduction. Wiley, Chichester, Hoboken, NJ (**2004**).
3. L. Pavesi and D. J. Lockwood, Silicon Photonics, Springer-Verlag Berlin Heidelberg (**2004**).
4. L. Canham, *Appl. Phys. Lett.* 57, 1046 (**1990**).
5. W. X. Zhu, Y. X. Gao, L. Z. Zhang, J. C. Mao, B. R. Zhang, J. Q. Duan, and G. G. Qin, *Superlattices and Microstruct.* 12, 409 (**1992**).
6. M. A. Tischler, R. T. Collins, J. H. Stathis, and J. C. Tsang, *Appl. Phys. Lett.* 60, 639 (**1992**).
7. J. C. Vial, A. Bsiesy, F. Gaspard, R. Hérino, M. Ligeon, F. Muller, and R. Romestain, R. M. Macfarlane, *Phys. Rev. B* 45, 14171 (**1992**).
8. J. Q. Duan J. C. Mao, L. Z. Zhang, B. R. Zhang, and G. G. Qin, *J. Infrared Millim. Wave* 11, 401 (**1992**).
9. L. Pavesi, L. Dal Negro, C. Mazzoleni, G. Franzó, and F. Priolo, *Nature* 408, 440 (**2000**).
10. B. Gelloz and N. Koshida, *J. Appl. Phys.* 88, 4319 (**2000**).
11. H. Takagi, H. Ogawa, Y. Yamazaki, A. Ishizaki, and T. Nakagiri, *Appl. Phys. Lett.* 56, 2379 (**1990**).
12. J. P. van der Ziel, R. Dingle, R. C. Miller, W. Wiegmann, and W. A. Nordland, Jr., *Appl. Phys. Lett.* 26, 463 (**1975**).
13. D. J. DiMaria, J. R. Kirtley, E. J. Pakulis, D. W. Dong, T. S. Kuan, F. L. Pesavento, T. N. Theis, and J. A. Cutro, *J. Appl. Phys.* 56, 401 (**1984**).
14. X. L. Zheng, W. Wang, and H. C. Chen, *Appl. Phys. Lett.* 60, 986 (**1992**).
15. Y. Kanemitsu, K. Suzuki, H. Uto, Y. Masumoto, T. Matsumoto, S. Kyushin, K. Higuchi, and H. Matsumoto, *Appl. Phys. Lett.* 61, 2448 (**1992**).
16. Y. Kanemitsu, H. Uto, Y. Masumoto, T. Matsumoto, T. Futagi, and H. Mimura, *Phys. Rev. B* 48, 2827 (**1993**).
17. G. G. Qin, H. Z. Song, B. R. Zhang, J. Lin, J. Q. Duan, and G. Q. Yao, *Rev. B* 54, 2548 (**1996**).
18. I. M. Chang and Y. F. Chen, *Appl. Phys.* 82, 3514 (**1997**).
19. L. Canham, Properties of Porous Si, INSPEC, London (**1997**), p. 247.
20. G. G. Qin and Y. Q. Jia, *Solid State Commun.* 86, 559 (**1993**).
21. W. L. Wilson, P. F. Szajowski, and L. E. Brus, *Science* 262, 1242 (**1993**).
22. Y. H. Xie, M. S. Hybertsen, W. L. Wilson, S. A. Ipri, G. Carver, W. L. Brown, E. Dons, B. E. Weir, A. R. Kortan, G. P. Watson, and A. J. Liddle, *Phys. Rev. B* 49, 5386 (**1994**).
23. S. M. Prokes, *Appl. Phys. Lett.* 62, 3244 (**1993**).
24. S. Godefroo, M. Hayne, M. Jivanescu, A. Stemans, M. Zacharias, O. I. Lebedev, G. Van Tendeloo, and V. V. Moshachalkov, *Nat. Nanotechnol.* 3, 174 (**2008**).
25. M. Hayne, J. Maes, S. Bersier, M. Henini, L. Muller-Kirsch, R. Heitz, D. Bimberg, and V. V. Moshchalkov, *Physica B* 346–347, 421 (**2004**).
26. S. N. Walck and T. L. Reinecke, *Phys. Rev. B* 57, 9088 (**1998**).
27. A. G. Cullis, L. T. Canham, G. M. Williams, P. W. Smith, and O. D. Dosser, *J. Appl. Phys.* 75, 501 (**1994**).
28. A. G. Cullis, L. T. Canham, and P. D. Calcott, *J. Appl. Phys.* 82, 909 (**1997**).
29. M. V. Wolkin, J. Jorne, P. M. Faucher, G. Allan, and C. Delerue, *Phys. Rev. Lett.* 82, 197 (**1999**).
30. G. Qin and G. G. Qin, *J. Appl. Phys.* 82, 2572 (**1997**).
31. G. Qin, G. G. Qin, and S. H. Wang, *J. Appl. Phys.* 85, 6738 (**1999**).
32. G. G. Qin and Y. J. Li, *Phys. Rev. B* 68, 085309 (**2003**).
33. X. X. Wang, J. G. Zhang, L. Ding, B. W. Cheng, W. K. Ge, J. Z. Yu, and Q. M. Wang, *Phys. Rev. B* 72, 195313 (**2005**).
34. H. J. Xu and X. J. Li, *Opt. Express* 16, 2933 (**2008**).
35. A. G. Cullis, L. T. Canham, G. M. Williams, P. W. Smith, and O. D. Dosser, *J. Appl. Phys.* 75, 493 (**1994**).

36. G. G. Qin, X. S. Liu, S. Y. Ma, J. Lin, G. Q. Yao, X. Y. Lin, and K. X. Lin, *Phys. Rev. B* 55, 12876 (**1997**).
37. G. G. Qin, J. Lin, J. Q. Duan, and G. Q. Yao, *Appl. Phys. Lett.* 69, 1689 (**1996**).
38. G. G. Qin, *Mater. Res. Bull.* 33, 1857 (**1998**).
39. O. Savchyn, F. R. Ruhge, P. G. Kik, R. M. Todi, K. R. Coffey, H. Nukala, and H. Heinrich, *Phys. Rev. B* 76, 195419 (**2007**).
40. A. Ritcher, P. Steiner, F. Kozlowski, and W. Lang, *IEEE Electron Device Lett.* 12, 691 (**1991**).
41. N. Koshida and H. Koyama, *Appl. Phys. Lett.* 60, 347 (**1992**).
42. A. Halimaoui, C. Oules, G. Bomchil, A. Bsiesy, F. Gaspard, R. Herino, M. Ligeon and F. Muller, *Appl. Phys. Lett.* 59, 304 (**1991**).
43. L. T. Canham, W. Y. Leong, M. I. J. Beale, T. I. Cox, and L. Taylor, *Appl. Phys. Lett.* 61, 2563 (**1992**).
44. P. M. M. C. Bressers, J. W. J. Knapen, E. A. Meulenkamp, and J. J. Kelly, *Appl. Phys. Lett.* 61, 108 (**1992**).
45. A. Bsiesy, F. Muller, M. Ligeon, F. Gaspard, R. Herino, R. Romestain, and J. C. Vial, *Phys. Rev. Lett.* 71, 637 (**1993**).
46. H. Kandeko, P. J. French, and R. F. Wolffenbuttel, *J. Lumin.* 57, 101 (**1993**).
47. G. G. Qin, Y. M. Huang, L. Z. Zhang, B. Q. Zong, and B. R. Zhang, *Superlatt. Microstruct.* 16, 387 (**1994**).
48. G. G. Qin, A. P. Li, B. R. Zhang, and B. C. Li, *J. Appl. Phys.* 78, 2006 (**1995**).
49. G. G. Qin, A. P. Li, and Y. X. Zhang, *Phys. Rev. B* 54, R1122 (**1996**).
50. S. Y. Ma, B. R. Zhang, G. G. Qin, Z. C. Ma, W. H. Zong, and X. T. Meng, *Mater Res. Bull.* 32, 1427 (**1997**).
51. G. F. Bai, A. P. Li, Y. X. Zhang, Y. K. Sun, S. Y. Ma, G. G. Qin, Z. C. Ma, and W. H. Zong, *Phys. Low Dimension Structures* 1, 127 (**1998**).
52. L. S. Liao, X. M. Bao, N. S. Li, X. Q. Zheng, N. B. Min, *Solid State Commun.* 97, 1039 (**1996**).
53. J. Yuan and D. Haneman, *J. Appl. Phys.* 86, 2358 (**1999**).
54. J. Yuan, D. Haneman, I. Andrienko, R. Siegele, and P. Evans, *Semicond. Sci. Technol.* 13, 615 (**1998**).
55. L. Heikkila, T. Kuusela, and H. P. Hedman, *J. Appl. Phys.* 89, 2179 (**2001**).
56. X. M. Wu, Y. M. Dong, L. J. Zhuge, C. N. Ye, N. Y. Tang, Z. Y. Ning, W. G. Yao, and Y. H. Yu, *Appl. Phys. Lett.* 78, 4121 (**2001**).
57. M. J. Lu, X. M. Wu, and W. G. Yao, *Mat. Sci. Eng. B* 100, 152 (**2003**).
58. G. G. Qin, Y. Q. Wang, Y. P. Qiao, and B. R. Zhang, Z. C. Ma, and W. H. Zong, *Appl. Phys. Lett.* 74, 2182 (**1999**).
59. G. G. Qin, Y. Chen, G. Z .Ran, B. R. Zhang, S. H. Wang, G. Qin, Z. C. Ma, W. H. Zong, and S. F. Ren, *J. Phys.: Condens. Matter.* 13, 11751 (**2001**).
60. M. Fujii, M. Yoshida, Y. Kanzawa, S. Hayashi, and K. Yamamoto, *Appl. Phys. Lett.* 71, 1198 (**1997**).
61. L. Tsybeskov, S. P. Duttagupta, K. D. Hirschman, P. M. Fauchet, K. L. Moore, and D. G. Hall, *Appl. Phys. Lett.* 70, 1790 (**1997**).
62. G. Z. Ran, Y. Chen, W. C. Qin, J. S. Fu, Z. C. Ma, H. Lu, J. Qin, W. H. Zong, and G. G. Qin, *J. Appl. Phys.* 90, 5835 (**2001**).
63. Y. Chen, G. Z. Ran, L. Dai, B. R. Zhang, G. G. Qin, Z. C. Ma, and W. H. Zong, *Appl. Phys. Lett.* 80, 2496 (**2002**).
64. D. Pacifcia, A. Irrera, G. Franzo, M. Miritello, F. Iacona, and F. Priolo, *Physica E* 16, 331 (**2003**).
65. A. Irrera, G. Franzo, F. Iacona, A. Canino, G. Di Stefano, D. Sanfilippo, A. Piana, P. G. Fallica, and F. Priolo, *Physica E* 38, 181 (**2007**).
66. M. E. Castagna, S. Coffa, M. Monaco, L. Caristia, A. Messina, R. Mangano, and C. Bongiorno, *Physica E* 16, 547 (**2003**).
67. J. M. Sun, W. Skorupa, T. Dekorsy, M. Helm, and A. N. Nazarov, *Opt. Mat.* 27, 1050 (**2005**).
68. A. Nazarov, J. M. Sun, W. Skorupa, and R. A. Yankov, *Appl. Phys. Lett.* 86, 151914 (**2006**).
69. F. Iacona, D. Pacifici, A. Irrera, M. Miritello, G. Franzo, F. Priolo, D. Sanfilippo, G. Di Stefano, and P. G. Fallica, *Appl. Phys. Lett.* 81, 3242 (**2002**).
70. K. Sun, W. J. Xu, B. Zhang, L. P. You, G. Z. Ran, and G. G. Qin, *Nanotechnology* 19, 105708 (**2008**).
71. A. V. Anikeenko and N. N. Medvedev, *Phys. Rev. Lett.* 98, 235504 (**2007**).


Received: 31 December 2008. Accepted: 31 March 2009.